PASSIVE AERODYNAMIC STABILIZATION OF A LOW EARTH ORBIT SATELLITE

T. Bak, R. Wisniewski

Institute of Electronic Systems
Aalborg University
DK-9220 Aalborg Ø, Denmark
email {tb,raf}@control.auc.dk

ABSTRACT

This paper discusses the influence of aerodynamic drag torque on the dynamics of a satellite in a very low altitude orbit.

The larger atmospheric density in low altitude earth orbits results in significant aerodynamic drag torques acting on the satellite. With a conventional satellite design this may result in instability. This paper shows how the instability can be avoided, and how the aerodynamic drag can be used for passive attitude stabilization of a satellite with an appropriate geometry.

Design recommendations and tradeoffs are presented for the use of aerodynamic drag in attitude control.

The results have been applied on a ESA study satellite required in an orbit with less than 250 km altitude. Simulations and analytical results indicate that the satellite will oscillate between two attitude equilibria. Performance of a basic attitude control algorithm providing stable satellite motion is given.

1. INTRODUCTION

Passive stabilization of satellites based on aerodynamic drag torques could be a desirable low cost, low weight control principle for future low altitude missions.

With an appropriate design the motion of the satellite can be controlled taking advantage of the aerodynamic drag while maintaining lifetime.

The work presented here is motivated by the ESA study satellite GSO-L (Global Space Observatory - Low). GSO-L is required in a low earth orbit (lower than 250 km) to meet science objectives related to studies of the lithospheric fields in the earth's crust. The influence of the aerodynamic drag is the major design issue when selecting an appropriate attitude control principle and nominal attitude for a satellite in this kind of orbit (see [1]).

Aero-stabilization has previously been addressed in [2] for the shuttle Hitchhiker GAMES mission. The results were focused on the effect of altitude decay and did not consider gravity gradient or shadowing.

For magnetic missions like GSO-L an instrument boom is often required and gravity gradient becomes an important factor. This paper investigates the gravity gradient, aerodynamic torque interaction and their influence on passive stabilitzation. Small angle uncontrolled equations of motion are derived indicating motion about two attitude equilibria. The analysis is followed by a study of of Mathieu-Hill equations describing the resonances due to variations in the atmospheric density and local winds. Design recommendations and tradeoffs imposed by aero-stabilization are presented.

The results are applied in the GSO-L satellite study resulting in a nominal GSO-L attitude where a field sensor boom is carried in the wake. The result is low drag forces while aerodynamic drag torques are used for compensating gravity gradient effects providing a passive stabilization of the satellite. Simulations show the estimated performance of a basic control algorithm.

The paper demonstrates the feasibility of passive aero-stabilization and provides guidelines for the satellite design to obtain the best attitude performance without sacrificing satellite lifetime.

2. SATELLITE DYNAMICS WITH AIR DRAG

Before progressing with the analysis orbit and body reference frames are defined. The orbit frame is defined with the nadir as the z_o axis, the y_o axis is perpendicular to the orbital plane pointing in the direction of negative angular momentum. The primary axis (x_o axis) is in the orbit plane in the direction of orbital motion. The satellite body frame is assumed aligned with the principal axes of inertia. Attitude is expressed as a 312 (yaw, roll, pitch) Euler rotation sequence from the orbit reference frame.

In general the dynamics relates torques acting on the satellite to the satellite angular velocity. The nonlinear equation of motion for a satellite in low earth orbit, (see [3]), is

$$I\,{}^b\dot{\mathbf{\Omega}}_{bw}(t) = -{}^b\mathbf{\Omega}_{bw}(t) \times (\mathbf{I}\,{}^b\mathbf{\Omega}_{bw}(t) + \mathbf{h}(t)) - \dot{\mathbf{h}}(t) + {}^b\mathbf{N}_{aero}(t) + {}^b\mathbf{N}_{gg}(t) + {}^b\mathbf{N}_{ctrl}(t), \quad (1)$$

where ${}^b\mathbf{\Omega}_{bw}$ is the satellite angular velocity with respect to an inertial frame, and $\mathbf{I}$ is the moments of inertia tensor (including wheel mass). The net angular momentum due to rotation of wheels relative to the satellite is denoted $\mathbf{h}$. The torques represented in Eq. (1) are: the aerodynamic

drag torque, $\mathbf{N}_{aero}$, the gravity gradient torque, $\mathbf{N}_{gg}$, and control torque, $\mathbf{N}_{ctrl}$.

In the 200 km altitude region, aerodynamic drag is usually the dominant disturbance torque. For a small, relatively symmetric satellite with an instrument boom, however, the gravity gradient and drag torques may be equally important.

2.1. Gravity Gradient

Assuming a near-circular orbit and a satellite whose body axis coincide with the principal axis, the gravity gradient torque for small ψ (yaw), θ (pitch), and ϕ (roll) can be approximated by

$$\mathbf{N}_{gg} = -3\omega_o^2 \left[(I_y - I_z)\phi \mathbf{i}_b + (I_x - I_z)\theta \mathbf{j}_b\right] \quad (2)$$

where the $\mathbf{i}_b, \mathbf{j}_b, \mathbf{k}_b$ unit vector set defines the satellite body frame and I_x, I_y, I_z are the principal moments of inertia, ω_o is the orbital rate.

2.2. Aerodynamic Drag Torque

Impact of the atmosphere molecules on the satellite's surfaces induces forces and torques about the centre of mass. Assuming that the energy of the molecules is totally absorbed on impact with the spacecraft, the force $d\mathbf{f}_{aero}$ acting on one surface element dA is described by (see [3]):

$$d\mathbf{f}_{aero} = -\frac{1}{2} C_D \rho v^2 (\hat{\mathbf{n}} \cdot \hat{\mathbf{v}}_b) \hat{\mathbf{v}}_b dA, \quad (3)$$

where dA is a surface element, $\hat{\mathbf{n}}$ is an outward normal to the surface, $\hat{\mathbf{v}}_b$ is a unit vector in the direction of the translational velocity in the body frame. ρ is the atmospheric density, and C_D is the drag coefficient. The total aerodynamic force is determined by integrating over the spacecraft surface.

By approximating the a satellite structure by a collection of simple geometrical elements the aerodynamic torque can be found as the vector sum of the torques on the individual elements composing the satellite surface

$$\mathbf{N}_{aero} = \sum_{i=1}^{k} \mathbf{r}_i \times \mathbf{F}_i, \quad (4)$$

where $\mathbf{r}_i$ is the vector from the spacecrafts centre of mass (CM) to the centre of pressure (CP) of the i*th* element. $\mathbf{F}_i$ is the integration of Eq. (3) over the individual elements.

To simplify the expression in Eq. (4) assume that the satellite is modelled as a number of plane surfaces. Eq. (4) then becomes

$$\mathbf{N}_{aero} = \frac{1}{2} C_D \rho v^2 \sum_{i=1}^{k} A_i (\hat{\mathbf{n}}_i \cdot \hat{\mathbf{v}}_b) \hat{\mathbf{v}}_b \times \mathbf{r}_i \quad (5)$$

where A_i is the surface areas.

Drag force acts along the negative velocity (ram) vector. For a circular orbit the ram vector is approximately given by the x_o axis. Using the 312 Euler sequence and assuming small angles $\hat{\mathbf{v}}_b$ can be appproximated by

$$\hat{\mathbf{v}}_b = \mathbf{A}_{bo} \hat{\mathbf{v}}_o = -\mathbf{A}_{bo} \mathbf{i}_o \approx -\mathbf{i}_b + \psi \mathbf{j}_b - \theta \mathbf{k}_b \quad (6)$$

Using Eq. (6) in Eq. (5) results in a small angle model of aerodynamic drag.

2.3. High Fidelity Models

The small angle models given above are used in analysis. Simulation, however, is based on high fidelity models of satellite dynamics and environmental disturbances. Of particular interest here are the models of atmospheric densities and winds.

The atmospheric density is modelled based on MSIS-86 [4]. MSIS-86 is an empirical model of the neutral temperature and density in the thermosphere and lower exosphere (86 to 2000 km) and it provides small frequency atmospheric disturbances ie. $\rho(t)$.

Higher frequency contributions are modelled using a local wind model, HWM-93 [5]. HWM-93 is an empirical model of the horizontal neutral wind in region 0-2000 km.

3. UNCONTROLLED PITCH DYNAMICS

To simplify the analysis the satellite surfaces is lumped into three perpendicular planes with areas A_1, A_2 and A_3. The x_b, y_b and z_b axes are normal to the surfaces with areas A_1, A_2 and A_3 respectively. Neglecting shadowing, and omitting second order terms Eq. (5) and Eq. (6) can be combined as

$$\begin{aligned} \mathbf{N}_{aero} &= \frac{1}{2} C_D \rho v^2 [A_1(-\psi r_{1z} - \theta r_{1y})\mathbf{i}_b \\ &+ (\theta r_{1x} - r_{1z})\mathbf{j}_b + (r_{1y} + \psi r_{1x})\mathbf{k}_b) \\ &+ A_2(\psi r_{2z}\mathbf{j}_b - \psi r_{2y}\mathbf{k}_b) \\ &+ A_3(\theta r_{3z}\mathbf{j}_b - \theta r_{3y}\mathbf{k}_b)] \end{aligned} \quad (7)$$

where $\mathbf{r} = [r_{1x}, r_{1y}, r_{1z}]^T$ is the CM-CP vector for surface A_1 etc.

Crosscoupling in Eq. (7) can be minimized by an appropriate symmetric design. Designing the satellite with the CP of the A_1 surface on the x_b and all surfaces summetric about their normal vector nulls r_{1z}, r_{1y}, r_{2z}, and r_{3y}. As a result roll is removed from the system, and pitch and yaw are decoupled, thereby simplifying the dynamics considerably.

For a magnetic field observing satellite like GSO-L an instrument boom is necessary to remove instruments from the electromagnetic contamination of the satellite main

body. The boom will determine the axis of least moment of inertia. Placing the boom along the ram vector reduces the total area perpendicular to the ram vector thereby optimizing with respect to orbital lifetime. The satellite structure is hence foreseen as indicated in Figure 1.

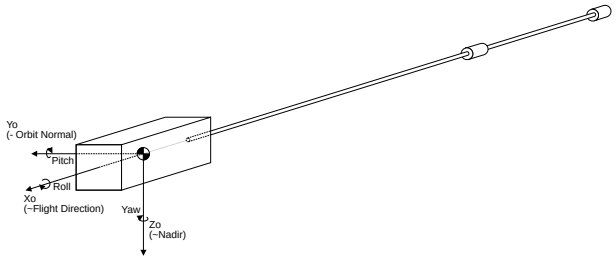

Figure 1: *Sketch of GSO-L spacecraft structure*.

Removing the crosscupling and roll dependency from Eq. (7) the interaction with gravity gradient can be investigated by looking at the pitch dynamics only. Combining the gravity gradient and aerodynamic torques results in the uncontrolled pitch dynamics

$$I_y\ddot{\theta} = \left(3\omega_o^2(I_z - I_x) + \frac{1}{2}C_D\rho v^2(A_1 r_{1x} + A_3 r_{3z})\right)\theta. \tag{8}$$

3.1. Stability of Pitch Dynamics

With an attitude as shown in Figure 1 the smallest moment of inertia is I_x and the gravity gradient becomes positive in Eq. (8). Without the aerodynamic torque the system is therefore characterized by the ustable gravity gradient poles. Gravity gradient will tend to point the axis of least moment of inertia towards nadir or zenith.

Drag forces applied behind the CM (ie. negative r_{1z} or r_{3z} counterbalance the gravity gradient and moves the poles to the imaginary axis resulting in a marginally stable system.

The condition for marginal stability is hence

$$A_1 r_{1x} + A_3 r_{3z} < -\frac{6\omega_o^2(I_z - I_x)}{C_D\rho v^2} \tag{9}$$

The inequality is implemented by a proper selection of $A_1 r_{1x} + A_3 r_{3z}$ or by decreasing the inertia and increasing the atmospheric density. The natural frequency of the marginally stable system is typically low making the system slowly oscillating. The oscillation can therefore be damped by a controller low bandwidth. A negative CM-CP offset is difficult to achieve, but may partly be realized taking into consideration the aerodynamic shadowing.

3.2. Aerodynamic Shadowing

Aerodynamic shadowing by the ram surface will reduce the drag effects on structural elements in the wake (ie. the boom on GSO).

The effect of shadowing from the ram surface was modelled in a simulation as a box shaped volume behind the surface with zero atmospheric density. The result is a nonlinear equation describing the torque applied to the system. Integrating the negative torque yields the potential energy of the nonlinear pitch system under influence of gravity gradient, aerodynamic drag and shadowing as shown in Figure 2.

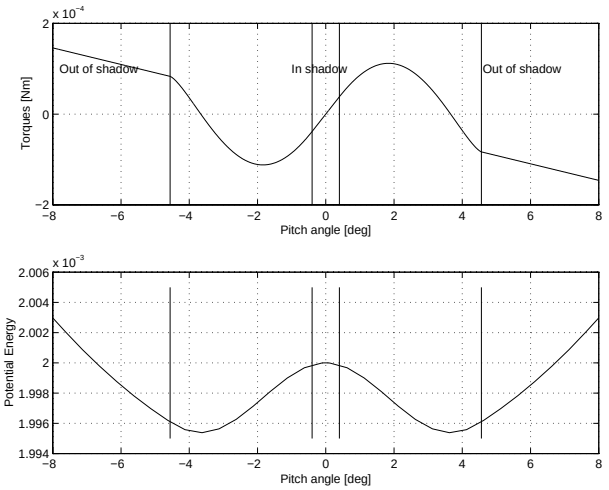

Figure 2: *Torques and potential energy of pitch system under influence of gravity and aerodynamic drag/shadowing. Based on GSO-L geometry and mass properties.*

The torque plot on Figure 2 illustrates the torque dependency of pitch angle. With the boom in shadow the slope of the torque curve is determined by gravity gradient and drag on the ram surface (positive CM-CP). The result is an unstable system. As the boom moves out of the shadow drag torques from the boom become increasingly dominating and the result is a marginally stable system (for pitch $>$3.6 degree).

The potential energy curve indicates an oscillatory behaviour as expected of a marginally stable system. The nominal attitude (0 degree pitch) is unstable. The two equilibria around approximately 3.6 degrees are marginally stable and separated by a potential barrier. For large initial errors (ie. $>$ 7 degrees) the satellite attitude will oscillate about the nominal attitude. Smaller initial errors will lead to oscillations about one of the 3.6 degrees equilibria as the satellite cannot pass the potential barrier.

The equilibria are determined by zero crossing of the torque curve and its negative gradient. The zero crossing of the torque curve is characterized by the gravity gradient plus a ram and boom area tradeoff.

The effective A_1 area is made up of contributions from the boom segments and the ram surface. It is clear that

to achieve a negative r_{1x} the contribution from the ram surface must be minimized. By adopting a spherical ram surface with centre of the sphere in the CM the surface normal is parallel to the CM-CP line resulting in a zero torque (see Eq. (5)) contribution from the ram area. A partial effect could be achieved by rounding the corners of the ram surface.

It should be noted that the perfect shadowing assumed here is not accurate. The assumed vacuum behind the ram surface will tend to fill up causing drag on the boom and its platforms. It will increase aerodynamic forces and thereby decrease lifetime, but it has a positive effect on attitude performance. Reduced shadowing will decrease the CM-CP offset lowering the equilibrium angle and thereby improve attitude performance.

4. PARAMETRIC ATTITUDE RESONANCES

Another possible source of instability is related to parametric resonances caused by higher order density harmonics and local wind.

Ignoring the slow increase in density due to altitude decay, the density profile is modelled as a bias term ρ_0 and harmonic terms of the orbit frequency ω_o

$$\rho(t) = \rho_0 + \sum_{i=1}^{\infty} \rho_i \cos(i\omega_o t). \tag{10}$$

Substituting $\rho(t)$ into Eq. (8) enables us to represent Eq. (8) in the form of the Hill equation

$$\ddot{\theta} + \Omega^2 \left[1 + 2\sum_{i=1}^{\infty} \mu_i cos(i\omega_o t)\right] \theta = 0, \tag{11}$$

where the natural frequency of oscillation Ω is given by

$$\Omega = \sqrt{\frac{-3\omega_o^2(I_z - I_x) - \frac{1}{2}C_D\rho_0 v^2(A_1 r_{1x} + A_3 r_{3z})}{I_y}} \tag{12}$$

and the excitation parameter μ_i is

$$2\mu_i = \frac{C_D\rho_i v^2(A_1 r_{1x} + A_3 r_{3z})}{C_D\rho_0 v^2(A_1 r_{1x} + A_3 r_{3z}) + 6\omega_o^2(I_z - I_x)} \tag{13}$$

For GSO in a 200 km orbit a typical value for μ_1 is 0.18. In general the magnitude of μ_i reduces as i increases. To avoid problems in Eq. (12) it is assumed that the aerodynamic drag torque dominate the gravity gradient torque.

For $i = 1$ Eq. (11) is known as the Mathieu equation and for small values of μ_1 instability regions occur at the following frequencies (see [6])

$$\omega_* = \frac{2\Omega}{k}, \quad (k = 1, 2, 3, \ldots) \tag{14}$$

Eq. (14) gives the relationship between the frequency of the external aerodynamic torque (ω) and the frequency of the satellite motion (Ω), near which instability is possible. Parametric resonances occur when the exciting frequency is equal to the double of the natural frequency. The number k determines the first, second, etc. regions of instability. The first three regions of instability on the plane $(\mu_1, \omega/\Omega)$ are shown in Figure 3 [6].

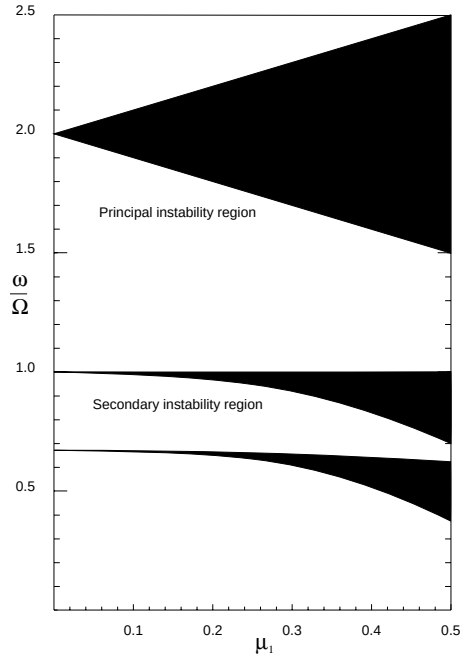

Figure 3: *First three instablity regions on the plane* $(\mu_1, \omega/\Omega)$. *Black areas indicate instability regions.*

As the altitude decreases, the natural frequency Ω increases due to increased bias drag. As a result ω/Ω decreases and the satellite dynamics traverses stable and unstable regions over time.

4.1. Atmospheric Density FFT

A Fast Fourier Transform (FFT) of the atmospheric density in a nominal GSO-L orbit indicates significant frequency components of up to five times the orbital frequency, corresponding to $i = 1, 2, \ldots, 5$ in Eq. (11). The cyclic component at the orbital rate is caused by the Earth's diurnal bulge, whereas the higher frequencies are mainly due to local winds. From Eq. (14) it is clear, that for $i = 2$ instablitity occur at

$$\omega_* = \frac{\Omega}{k}, \quad (k = 1, 2, 3, \ldots) \tag{15}$$

and the second instablity region of Eq. (14) becomes first region for $i = 2$. Similar analysis can be applied for the remaining frequency components.

To avoid parametric resonances it is desirable to keep the natural frequency Ω above the the principal instability region of the last significant frequency found through the

FFT analysis. For GSO this results in

$$\begin{aligned} \Omega &> \frac{5}{2}\omega_o \\ A_1 r_{1x} + A_3 r_{3z} &> -\frac{(\frac{5}{2})^2 \omega_o^2 I_y + 3\omega_o^2 (I_z - I_x)}{\frac{1}{2} C_D \rho_0 v^2} \end{aligned} \quad (16)$$

4.2. Design Guideline Summary

The above analysis of the passive aero-stabilization has resulted in several design guidelines summarized below.

- Crosscoupling is minimized by symmetric design. CP of the ram surface on the x_b principal axis and all surfaces symmetric about their normal vector simplifies dynamics considerably.
- Two explicit criterion for attitude stability were established in Eq. (9) and Eq. (16).

The criterion in the latter are possibly fullfilled through

- A large ρ_0 (lower orbit). Larger density does, however, reduce satellite lifetime.
- Minimizing ram surface drag contribution. Decreased drag torque from ram surface can be achieved though structural design (rounded corners) or by lowering the CM (ie. moving it closer to the ram surface).
- Increasing boom area or length increases the CM-CP offset but reduces lifetime.
- Decreasing inertia improves performance but reduces ballistic coefficient.

5. GSO-L CASE STUDY

A number of scenarios are presented in the following illustrating the aerodynmaic drag stabilization. Mass, orbit, and geometric properties are based on a particular design recommended for the proposed GSO-L satellite.

Table 1: *Summary of GSO-L orbit, mass, and structural properties. Empty propulsion tank.*

Orbit	
Altitude [km]	200.0
Inclination [deg.]	98.5
Period [min.]	88.3
Eccentricity	0.0
Ascending node	12.00h
Structural	
Moments of inertia [kg/m^2]	[21, 901, 901]
Main body [m]	$1.58 \times 0.71 \times 0.71$
Lower boom [m]	0.024×5.39
Upper boom [m]	0.024×2.00
Lower platform [m]	0.18×0.13
Upper platform [m]	0.585×0.32

5.1. Torque Budget

To assess the maximum aerodynamic torques the satellite was simulated in a zenith pointing mode (equivalent to satellite x-axis pointing at the zenith). Results are shown in Figure 4 for full and empty propulsion tanks. The frequency of the aerodynamic excitation is clearly a multiple of the orbital frequency justifying the parametric resonance analysis.

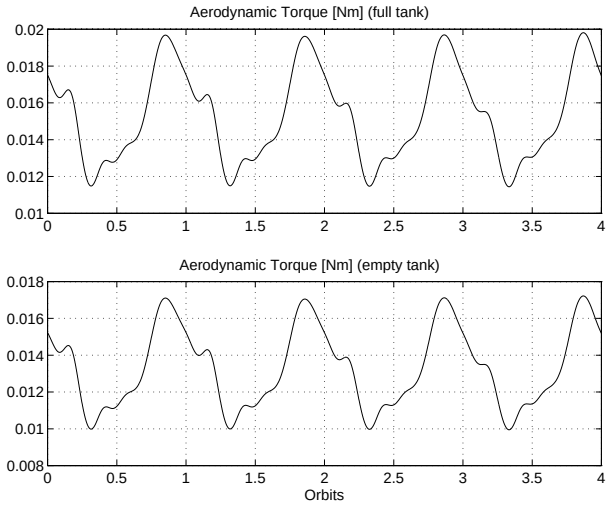

Figure 4: *Torques due to atmospheric drag for GSO-L. Full and empty tanks.*

5.2. Passive Stabilization

The GSO-L passive stabilization (uncontrolled dynamics) was investigated by simulations based on an initial 2 degree offset in pitch and a small angular velocity error. Figure 5 shows the cone angle (ie. the angle between body and orbit x axes and the magnitude of the angular velocity.

Only data for the empty tank scenario is presented. An increased CM-CP offset results in a larger torque contribution from the ram surface (due to increased CM relative to incident stream of atmpsphere molecules) making this a worst case situation from an aerodynamic drag point of view.

Note the influence of aerodynamic shadowing, ie. as the satellite rotates towards zero cone angle the boom moves into the shadow of the main body. The result is an increase in the destabilizing torques and by that an increased cone angle. As predicted the satellite oscillates about an equilibrium.

Equilibria at lower angles are observed in simulations. The discrepancy is due to variations in the atmospheric density and the surfaces omitted in the analysis.

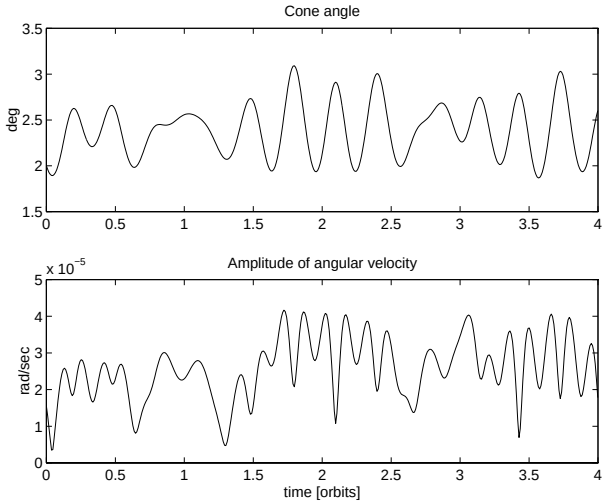

Figure 5: *Cone angle and angular velocity for the GSO-L in passive stabilization. Empty propulsion tank.*

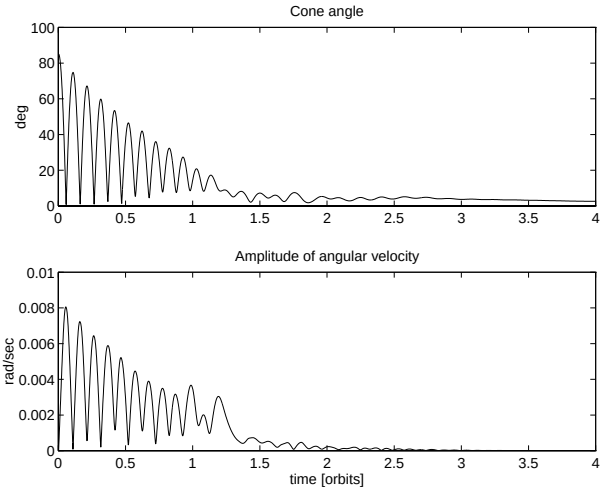

Figure 6: *Acquisition from zenith pointing attitude. Cone angle, and magnitude of angular velocity with reation wheel control.*

5.3. Acquisition

Aerodynamic drag and gravity gradient effects result in a system with roots in the right half plane or on the imaginary axis (unstable or marginally stable system behaviour). Including damping in the system moves the poles into the left half plane stabilizing the system.

Damping is introduced as a rate dependant term in Eq. (8). Physically an angular velocity dependant actuation device is recommended. Three or more reaction or momentum wheels will provide the necessary damping of the aerodynamic drag effects on pitch and yaw/roll motion.

To assess closed loop behaviour, a simple, proportional velocity feedback control law was simulated. Acquisition of the satellite from the worst case zenith pointing mode in the empty tank situation as shown in Figure 6.

From a 90 degree attitude error the satellite is acquired to within a cone angle of approximately 5 degrees. A position control loop besides the velocity control presented, would possibly stabilize the satellite with approximately a 0 degree cone angle.

6. CONCLUSION

The influence of aerodynamic drag on the dynamics of a sattellite in very low orbit was investigated. Based on analysis and simulations passive aerodynamic stabilization was proposed and the performance predicted.

Analysis of the small angle, unstable pitch dynamics lead to recommendations related to the structural design and a simple criteria for maginal pitch stability. An oscillatory behaviour about two equilibria was predicted. Parametric resonances was avoided by keeping the natural frequency of the satellite above the fifth region of instablity.

The analysis resulted in a number of design guidelines for the structural and mass properties of a aerodynamic stabilized satellite.

Simulations performed with GSO-L data demonstrated the feasibility of aerodynamic stabilization.

ACKNOWLEDGEMENTS

The research described in this paper was performed under contract no. 11334/95/NL/CN with the European Space Agency.

REFERENCES

1. Bak T & al Jun. 1996, Gso-l: Assesment of attitude dynamics, Tech. Rep. AAU/GSO/RPT/003-L ver. 1.3, Aalborg University.
2. Kumar R R & al 1995, Parametric and classical resonances in passive satellite aero-stabilization, in *ASS/AIAA Spaceflight Mechanics Meeting*.
3. Wertz J, editor 1978, *Spacecraft Attitude Determination and Control*, D. Reidel Publishing Co., Dordrecht.
4. Hedin A E 1987, Msis-86 thermospheric model, *J. Geophys. Res. 92*.
5. Hedin A E 1991, Revised global model of thermosphere winds using satellite and ground-based observations, *J. Geophys. Res. 96*, pp. 7657–7688.
6. Bolotin V 1964, *The Dynamic Stability of Elastic Systems*, Holden-Day.